80-MHz Intravascular Ultrasound Transducer Using PMN-PT Free-Standing Film

Xiang Li, *Student Member, IEEE*, Wei Wu, Youngsoo Chung, Wan Y. Shih, *Member, IEEE*, Wei-Heng Shih, Qifa Zhou, *Senior Member, IEEE*, and K. Kirk Shung, *Fellow, IEEE*

Abstract—$[Pb(Mg_{1/3}Nb_{2/3})O_3]_{0.63}[PbTiO_3]_{0.37}$ (PMN-PT) free-standing film of comparable piezoelectric properties to bulk material with thickness of 30 µm has been fabricated using a modified precursor coating approach. At 1 kHz, the dielectric permittivity and loss were 4364 and 0.033, respectively. The remnant polarization and coercive field were 28 µC/cm^2 and 18.43 kV/cm. The electromechanical coupling coefficient k_t was measured to be 0.55, which was close to that of bulk PMN-PT single-crystal material. Based on this film, high-frequency (82 MHz) miniature ultrasonic transducers were fabricated with 65% bandwidth and 23 dB insertion loss. Axial and lateral resolutions were determined to be as high as 35 and 176 µm. *In vitro* intravascular imaging on healthy rabbit aorta was performed using the thin film transducers. In comparison with a 35-MHz IVUS transducer, the 80-MHz transducer showed superior resolution and contrast with satisfactory penetration depth. The imaging results suggest that PMN-PT free-standing thin film technology is a feasible and efficient way to fabricate very-high-frequency ultrasonic transducers.

I. Introduction

I NTRAVASCULAR ultrasound (IVUS) has proven to be a valuable medical imaging modality for the diagnosis of arterial diseases. Its ability to directly image the vessel wall enables IVUS to provide precise evaluations of lumen dimensions, plaque composition, and calcium content [1]–[4]. A typical IVUS probe consists of a rotating shaft with a side-looking unfocused single-element transducer which provides a radial imaging geometry of a cross section of a vessel. The size of an IVUS catheter in clinical applications ranges from 2.6 to 3.6 Fr (0.90 to 1.18 mm), limiting the aperture of the transducer within the catheter to be less than 0.8 mm [3]. The center frequencies of commonly used IVUS transducers are between 20 and 40 MHz, implying that the axial/lateral resolutions are on the order of 60 to 300 µm. This value is inferior to that of intravascular optical coherence tomography (OCT) imaging, the resolution of which is on the order of 10 to 30 µm, providing much more detailed information about the microstructures of vessel and plaque compositions. However, the drawbacks of limited penetration depth of approximately 1 mm and the blood clearance safety issue prevent OCT from being efficiently used [5]–[8]. Increasing IVUS center frequency to 80 MHz or higher is a compromise between resolution and penetration. To date, little IVUS work has been done at such high frequencies, because it is hard to fabricate miniature transducers working well at 80 MHz or higher. Another concern is the strong tissue attenuation at high frequencies. At 80 MHz, an attenuation coefficient of 10 dB/mm is expected for the coronary artery, which means that a penetration depth of 3 mm can be achieved for a system with a dynamic range of 60 dB [3]. However, such a system requires highly sensitive miniaturized IVUS transducers, which is a great challenge.

Building such high-frequency transducers is challenging because the preparation of very thin piezoelectric layers with properties similar to the bulk material is difficult. The merit of the piezoelectric material is mostly determined by electromechanical coupling coefficient (k_t) and dielectric permittivity ($\varepsilon_r/\varepsilon_0$). Piezoelectric materials with high k_t value are efficient in energy conversion, suggesting improved sensitivity of the transducers. Meanwhile, dielectric permittivity is a critical issue considering the electrical impedance matching of the transducers to the 50-Ω imaging electronics, which would affect the sensitivity in both transmitting and receiving. The electrical impedance of a transducer is inversely proportional to the piezoelectric material's surface area and dielectric permittivity value [9]. For a miniaturized IVUS transducer, materials with high dielectric permittivity value are more desirable. Among all piezoelectric materials, $[Pb(Mg_{1/3}Nb_{2/3})O_3]_{0.63}[PbTiO_3]_{0.37}$ (PMN-PT) single crystal is a promising candidate with high k_t (0.58, HC materials, Bolingbrook, IL), $\varepsilon_r/\varepsilon_0$ (5229 [10]) and d_{33} (2000 pC·N^{-1} [11]) values. However, traditional lapping of PMN-PT single crystal bulk down to the thickness of 20 to 30 µm is extremely difficult and time consuming. Relatively large thickness variation (~3 µm) and cracking would make the quality of transducers hard to control. Additionally, the degradation of dielectric and electromechanical properties of single crystals with decreasing thickness [12] may decrease the sensitivity of a high-frequency transducer. A more feasible solution is to pursue piezoelectric thin film technology. In our previous work, sol-gel lead zirconate

titanate (PZT) and sputtered ZnO thin films have been investigated for fabrication of high-frequency (>80 MHz) ultrasonic transducers [13]–[16]. However, k_t values (~0.5) and sensitivities of sol-gel PZT transducers are relatively low. The drawbacks to using ZnO for active transducer elements are the relatively low k_t (~0.28) and $\varepsilon_r/\varepsilon_0$ (~8) values, which make them only suitable for fabricating large-aperture transducers.

PMN-PT thin films have been extensively studied [17]–[21]. Because of their high k_t and $\varepsilon_r/\varepsilon_0$ values, they could be good candidates for IVUS transducer fabrication. In this paper, we report the use of novel PMN-PT free-standing films for high-frequency transducers. In contrast to normal thin films that require substrates which degrade the piezoelectric properties of films, free-standing films were produced without substrate. Based on the films, highly sensitive miniaturized 80-MHz IVUS transducers were built. *In vitro* imaging of healthy rabbit aorta has been carried out to verify the feasibility of the thin-film transducers for intravascular imaging with better resolution than current transducers. It is shown that the use of piezoelectric free-standing films can be a viable approach to produce very-high-frequency ultrasound transducers and greatly simplify the process of preparing thin piezo-electric layers.

II. PREPARATION AND CHARACTERIZATION OF PMN-PT FREE-STANDING FILM

A. Film Fabrication

PMN-PT was synthesized with a modified precursor coating method as previously described [17]. Nb_2O_5 (99.99%, Aldrich Chemical Co., Milwaukee, WI), titanium isopro-poxide ($Ti(OCH(CH_3)_2)_4$, 99.9% Alfa Aesar, Ward Hill, MA), lead acetate anhydrous ($Pb(CH_3COO)_2 \cdot 2Pb(OH)_2$, Fluka, St. Louis, MO), $Mg(Ac)_2 \cdot 6H_2O$ (99.9%, Alfa Aesar), and NH_4OH (5M, Aldrich Chemical Co.) were used in this study.

0.1 mol of Nb_2O_5 powder was first suspended in 500 mL of distilled water, then ultrasonicated (Ultrasonic Homogenizer 4710 series, Cole-Parmer Instrument Co., Vernon Hills, IL) for 10 min to break up the Nb_2O_5 ag-glomerates. To precipitate $Mg(OH)_2$ onto the Nb_2O_5 sur-face, $Mg(CH_3COO)_2 \cdot 6H_2O$ (0.105 mol) was continuously dropped into the suspension during this coating process. NH_4OH (5M) was used to keep the pH level above 10.5 and the suspension was stirred for 30 min after mixing. The suspension was dried at 150°C by a hotplate. After drying, a precursor slurry was made from a lead acetate anhydrous ($Pb(CH_3COO)_2 \cdot 2Pb(OH)_2$) solution in ethyl-ene glycol (EG) ($HOCH_2CH_2OH$, Alfa Aesar) with 15% excess lead. The suspension was then dried at 230°C on a hot plate. Pyrochlore-free perovskite PMN powder was obtained by the dried PMN precursor powder, which was first heated at a rate of 1°C/min to 360°C for 2 h, followed by 5°C/min heating to 950°C for 2 h.
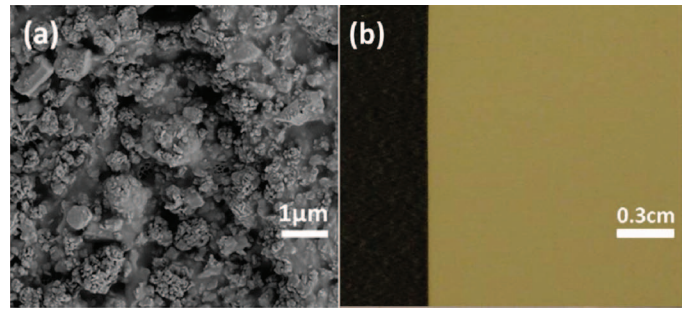

Fig. 1. (a) A scanning electron micrograph of the top surface of a PMN-PT green tape; (b) an optical image of a PMN-PT green tape on a black benchtop.

A PT precursor solution in EG with a stoichio-metric quantity of $Pb(CH_3COO)_2 \cdot 2Pb(OH)_2$ and $Ti(OCH(CH_3)_2)_4$ was prepared by dissolving in EG be-fore mixing. The perovskite PMN powder was then sus-pended in a PT precursor solution containing lead acetate and titanium isopropoxide ($Ti(OCH(CH_3)_2)_4$, 99.9% Alfa Aesar) in EG and ball-milled for 48 h. PMN-PT green powder was obtained by drying at 230°C (with constant stirring) followed by heat treatment at a rate of 1°C/min to 360°C for 2 h. After drying, the resultant powder was ball-milled again for 24 h to ensure intimate mixing of the PMN powder with the PT precursor, which was ready for tape casting. The size of the PMN and PT precursor par-ticles was 430 and 44 nm, respectively, by BET according to the previous study [17]. A scanning electron microscopy (SEM) micrograph of the green tape is shown in Fig. 1(a), where the submicron-sized PMN is intimately mixed with the nano-sized PT precursor. The tape casting process was carried out by Maryland Tape Casting Co. (Bel Air, MD). The solids loading and viscosity of the slurry had been optimized by adding binders and dispersants. The slurry was ball-milled for 48 h and vacuumed to remove bubbles before casting. The solids loading of the slurry was 60.74% by weight. The thickness of the tape is con-trolled by adjusting the gap of the doctor blade. The re-sultant tape was smooth, without warping or cracking, as shown in Fig. 1(b). The PMN-PT green tape was sintered at 1200°C for 2 h under saturated PbO vapor atmosphere at normal pressure to prevent the evaporation of Pb ele-ment from the PMN-PT tape.

B. Film Characterization

The crystalline phases of the sintered PMN-PT free-standing film were characterized by X-ray diffractom-etry (XRD), as shown in Fig. 2. The XRD pattern dis-played a pure perovskite phase, indicating that the film was well crystallized. The crystalline microstructures of the film were observed by SEM, shown in Fig. 3. The film was fully dense and without any crack or pore. Density was measured to be 7.76 g/cm³. Grain size was around 1 to 3 μm and film thickness was 30 μm. Ac-cording to [12], fine-grained PMN-PT films would offer
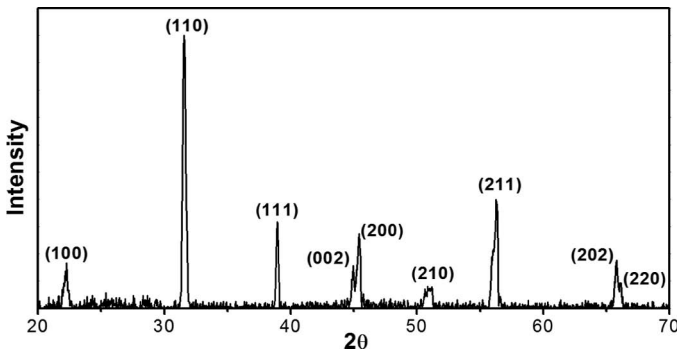
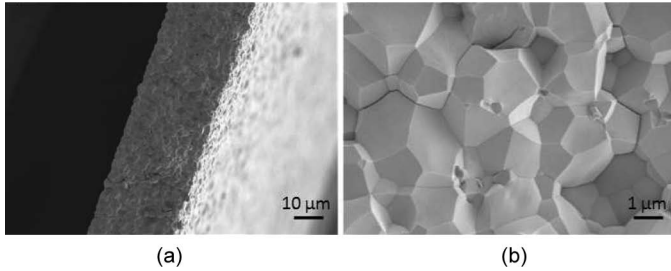Fig. 2. X-ray diffraction pattern of the PMN-PT free-standing film.

Fig. 3. Scanning electron micrographs of the PMN-PT free-standing film: (a) a cross-section view and (b) an enlarged view of the cross-section shown in (a).
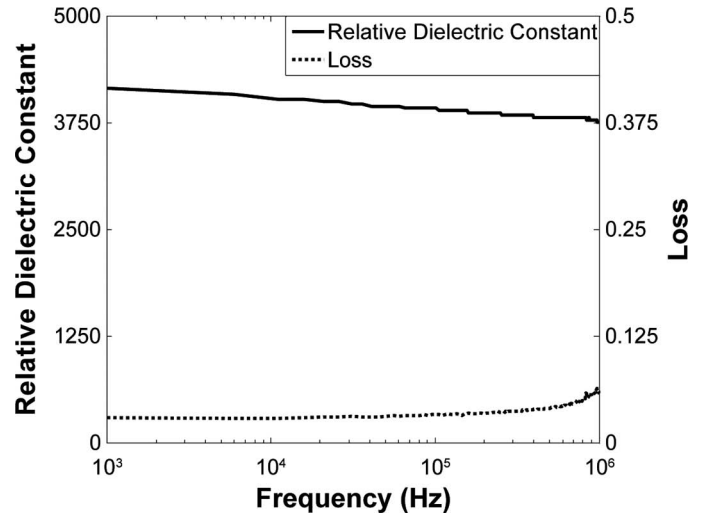

Fig. 4. Frequency dependence of dielectric constant and loss for PMN-PT film.
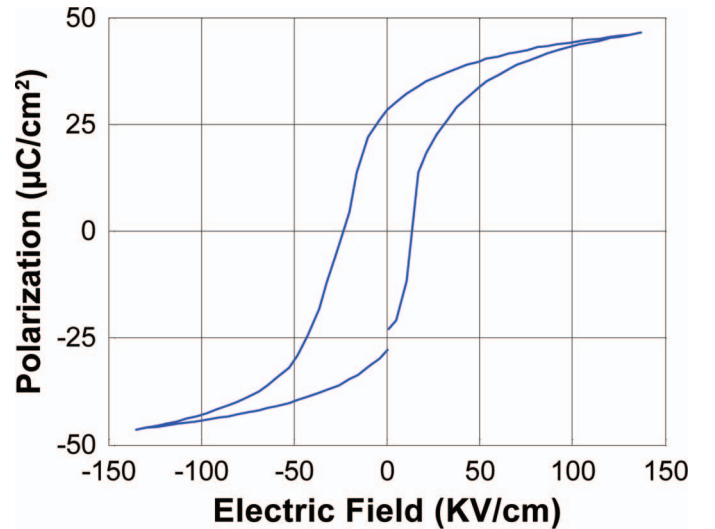
Fig. 5. Polarization-electric field hysteresis loop of the annealed PMN-PT free-standing film.

greater mechanical strength and improved property stability compared with coarse-grained (7 to 10 µm) PMN-PT ceramics.

For the measurement of electrical properties, 0.4 × 0.4 mm Cr/Au electrodes were sputtered onto the film as top electrodes. Another layer of Cr/Au was sputtered onto the bottom to serve as ground electrodes. Film samples were poled in a dc electric field of 30 kV/cm for 5 min at room temperature before measurements. The dielectric and ferroelectric properties were measured with an Agilent 4292A impedance analyzer (Agilent Technologies, Santa Clara, CA) and an RT6000 ferroelectric test system (Radiant Technology, Albuquerque, NM), respectively. The frequency dependence of the free relative dielectric permittivity ($\varepsilon_r/\varepsilon_0$) and the loss ($\tan\delta$) of the PMN-PT film were measured from 1 kHz to 1 MHz, as shown in Fig. 4. The $\varepsilon_r/\varepsilon_0$ and $\tan\delta$ at 1 kHz were found to be 4364 ($\pm$221) and 0.033 ($\pm$0.004), respectively. The $\varepsilon_r/\varepsilon_0$ and $\tan\delta$ values were close to those reported by Kosec (4100, 0.04) [10], Kuščer (3600, 0.036) [18], Uršič (3200) [19], and Calzada (1835, 0.04) [20], but were slightly inferior to those of bulk material (5229, 0.02) [10]. The high relative permittivity and low loss of the PMN-PT free-standing film implied a better electrical impedance match and improved sensitivity for miniature high-frequency transducers. The polarization-electric field hysteresis loop is shown in Fig. 5. The remnant polarization (P_r) and coercive field (E_c) were 28 µC/cm² (bulk, 12.3 to 33.1 µC/cm² [10]) and 18.43 kV/cm (bulk, 3.3 to 4.3 kV/cm [10]), respectively. The saturation po-

larization (P_s) was around 46 µC/cm² (Uršič, 40 µC/cm² [19]).

The frequency dependence of the electrical impedance and phase are displayed in Fig. 6, which shows that the electrical impedance at resonant peak is 29 Ω at 75 MHz, the series and parallel resonant frequencies are 69 and 80 MHz. k_t was calculated according to

$$k_t = \sqrt{\frac{\pi}{2} \cdot \frac{f_s}{f_p} \tan\left(\frac{\pi}{2} \cdot \frac{f_p - f_s}{f_p}\right)}, \tag{1}$$

where f_s and f_p are series and parallel resonant frequencies. The k_t value was found to be 0.55, which is comparable to the bulk PMN-PT single crystal (0.58, HC Materials, Bolingbrook, IL).
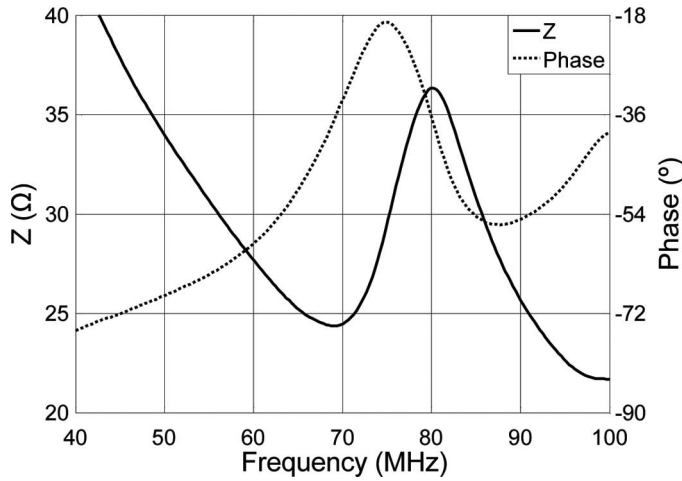
Fig. 6. Electrical impedance of PMN-PT free-standing film.

III. Fabrication and Characterization of High Frequency (80 MHz) Miniature Transducer

A. Transducer Fabrication

After characterization of the PMN-PT free-standing film, a 7 × 10 mm piece of film was used as the active piezoelectric layer to fabricate side-looking miniature transducers. A two-layer acoustic matching scheme was suggested to improve the performance of transducer [9]. Simulations on a Krimhotz–Leedom–Matthaei (KLM) equivalent circuit model (PiezoCad, Sonic Concepts, Woodinville, WA) predicted that 60% bandwidth at a center frequency of 81 MHz could be achieved by incorporating 4.4 μm silver epoxy (7.3 MRayl) and 1.8 μm Parylene (2.3 MRayl; Specialty Coating Systems, Indianapolis, IN) as first and second matching layers. However, even a 1-μm variation of the two layers would decrease the bandwidth by 20% or more. This made quality control in the fabrication process a great challenge.

The PMN-PT film was first sputtered with Cr/Au (500 Å/1000 Å) layers as electrodes at top and bottom. A silver epoxy matching layer made from Insulcast 501, sulcure 9 (American Safety Technologies, Roseland, NJ) and 0.5- to 1-μm silver particles (Sigma-Aldrich Inc., St. Louis, MO) was then cured over the top of the film and lapped to the designed thickness of 4.4 μm. However, because of the limitation of hand lapping, the variance of silver epoxy layer was ±3 μm. A conductive backing material, E-solder 3022 (VonRoll Isola, New Haven, CT) was then applied to the bottom of the film and lapped to 0.4 mm. The active stack was diced along the thickness direction into small posts with the aperture of 0.4 × 0.4 mm. The post was housed within a 0.57-mm ID polyimide tube (Small Parts Inc., Miramar, FL); an opening in the side of the tube allowed the transducer to face the side. A 0.25-mm OD electrical wire was connected to the conductive backing using E-solder 3022 inside the polyimide tube. The polyimide tube provided the electrical isolation from the outer stain-
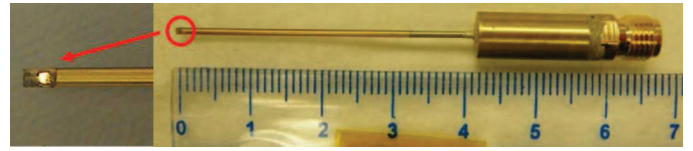

Fig. 7. Side-looking miniature transducer.

less steel needle housing. The outer needle housing, with an ID of 0.66 mm and OD of 0.92 mm, had a window on the side for the acoustic wave to go through. 5-min epoxy (Henkel Corporation, Irvine, CA) was used to fill the gap between the piezoelectric post and the needle housing to insulate the inner electrode. Another Cr/Au electrode was sputtered over the silver epoxy matching layer and the stainless steel needle housing to form the ground connection. A 2-μm-thick parylene layer (±0.5 μm) was vapor-deposited onto the transducer and needle housing to serve as a second matching and protecting layer. The transducer was finally connected to a brass holder and SMA connector for mechanical holding and electrical connection. To enhance the piezoelectric activity of the PMN-PT film, the finished transducer, shown in Fig. 7, was poled in a dc electric field of 30 kV/cm for 5 minutes at room temperature.

B. Transducer Characterization

The side-looking miniature transducers' performances were measured in a de-ionized water bath at room temperature. Pulse-echo tests [9] were conducted with X-cut quartz as a signal reflecting target. A single sinusoidal wave (80 MHz; 125% bandwidth; 42 V_{pp} and 200 Hz repetition rate) emitted from a monocycle function generator (Avtech Electrosystems Ltd., Ontario, Canada) was used to excite the transducers. Echo signals were amplified by a 33-dB pre-amplifier (MITEQ, Hauppauge, NY) and digitized by a 1-GHz oscilloscope (LC534, LeCroy Corp., Chestnut Ridge, NY). The frequency responses of the transducers were analyzed from the echo waveforms. The center frequency (f_c) and −6-dB fractional bandwidth (BW) could be determined by

$$f_c = \frac{f_l + f_u}{2} \tag{2}$$

$$\text{BW} = \frac{f_u - f_l}{f_c} \times 100\%, \tag{3}$$

where f_l and f_u are defined as lower and upper −6-dB frequencies, at which the magnitude of the amplitude in the spectrum is 50% (−6-dB) of the maximum. Fig. 8 shows a pulse-echo result from a representative transducer with matching layers that well-matched the designed parameters. Peak-to-peak amplitude was 573 mV. The measured center frequency was 82 MHz and the −6-dB fractional bandwidth was 65%. However, because of the difficulty in controlling the thickness of the silver epoxy matching
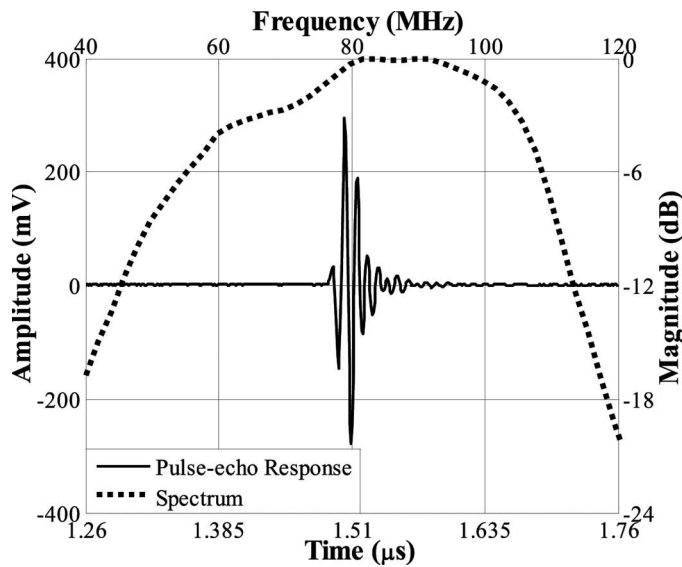
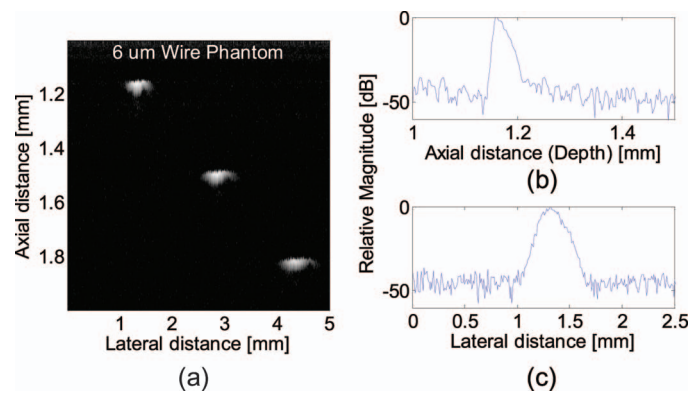Fig. 8. Pulse-echo measurement of one representative transducer.

Fig. 9. (a) Ultrasound wire phantom, displayed with a dynamic range of 45 dB; (b) axial and (c) lateral envelopes of echo signals from the wire located 1.2 mm away from the transducer surface.

layer, transducers with thinner layers (2 to 3 μm) possessed inferior bandwidths (35%) but slightly higher center frequencies (83 to 84 MHz), whereas transducers with thicker layers (5 to 7 μm) functioned at lower center frequencies (70 to 75 MHz) and had fair bandwidths (35 to 45%). The decrease in center frequency could be explained by the clamping and attenuation effects of matching layers.

Two-way insertion loss (IL) was calculated using the ratio of the frequency spectrum of the transmitted and received responses, which was compensated for the attenuation in water and loss caused by the imperfect reflection from the quartz target. The equation used was

$$\text{IL} = 20 \log \frac{V_\text{R}}{V_\text{T}} + 1.9 + 2.2 \cdot 10^{-4} \cdot 2d \cdot f_\text{c}^2, \qquad (4)$$

where V_T and V_R are the transmitting and receiving amplitudes, respectively, in volts; d is the distance in millimeters from the transducer to the target. The imperfect reflection from quartz crystal was compensated by 1.9 dB. The signal loss resulting from attenuation in water was compensated by $2.2 \cdot 10^{-4}$ dB/mm·MHz^2 [9]. The IL value was measured to be 23 dB at 80 MHz, which indicated the transducer's sensitivity is comparable with that of 80-MHz large-aperture LiNbO$_3$ single-crystal transducers, which have IL values of around 10 to 25 dB [9]. 6-μm-diameter tungsten wire targets were linearly scanned to determine axial and lateral resolutions of the transducer, as shown in Fig. 9(a). The envelopes, or point spread functions (PSFs), of echo signals from the wire located 1.2 mm from the transducer surface are displayed in Figs. 9(b) and 9(c). The axial and lateral resolutions were determined from the −6-dB envelope widths, which were 35 and 176 μm, respectively.

IV. IN VITRO INTRAVASCULAR IMAGING

In vitro imaging of a normal rabbit aorta was performed to test the side-looking PMN-PT free-standing film transducers' performance for intravascular imaging applications. During the experiment, the tip of the transducer was positioned inside the lumen of the sample, which was immersed in water and supported by a sponge to stand in a water tank. Only the part of the sample above the sponge was imaged. Circumferential scanning was achieved by rotating the water tank with the sample inside using a stepper motor (National Instruments, Austin, TX) while the transducer remained immobile. The same transmitting and receiving scheme was used for the pulse-echo tests, except higher driving voltages were used (up to 120 V$_\text{pp}$) and the RF data was digitized by a 12-bit data acquisition board (Gage Applied Technologies, Lockport, IL) with a sampling rate of 400 MHz. 1000 A-lines were acquired during each revolution and the scanning procedure was controlled by a customized LabVIEW program (National Instruments). RF data were saved and post-processed for image display. For comparison purposes, a 35-MHz PMN-PT single crystal transducer (60% bandwidth and 15 dB insertion loss) built using the same fabrication process with the same aperture size was used to image the same sample. All images were displayed with a 50 dB dynamic range.

Rabbit aorta images at 80 and 35 MHz were shown in Figs. 10(a) and 10(b), respectively. The 80-MHz image exhibited a much better resolution (denser speckles) than the 35-MHz image. Because of the improved resolution, the vascular wall and the surrounding fatty tissues in the 80-MHz image were better differentiated. The 80-MHz IVUS image could easily visualize the whole depth of vessel wall (up to 1.5 to 2 mm), though not the full depth of the hypoechoic fatty tissue. Because the healthy rabbit aorta vessel wall was relatively thin, it was not sufficient to fully evaluate the penetration depth.
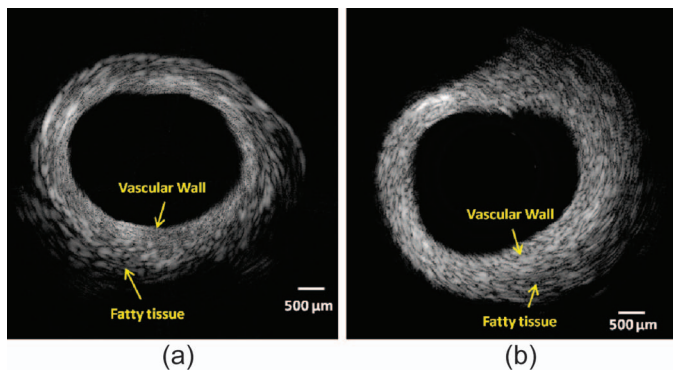
Fig. 10. Images of healthy rabbit aorta from (a) 80-MHz PMN-PT free-standing-film transducer; and (b) 35-MHz PMN-PT single-crystal transducer.

V. Conclusions

In this paper, we utilized the piezoelectric free-standing film technology for high-frequency (80 MHz) IVUS imaging. The PMN-PT free-standing film technology simplified the process of preparation of very thin layers of piezoelectric material with satisfactory quality, which is promising for very-high-frequency ultrasound applications. The fabrication procedures of a high-quality PMN-PT free-standing thin film without a substrate were presented. The measured dielectric and ferroelectric properties of the film were close to those of bulk material. Based on the film, miniature side-looking IVUS transducers were fabricated and tested. Testing results showed that the transducers had high resolution and sensitivity. An *in vitro* study was conducted with healthy rabbit aorta. The 80-MHz IVUS image demonstrated improved resolution and contrast to allow the differentiation of the vascular wall and surrounding fatty tissue, which could not be achieved by a 35-MHz transducer. As expected, the imaging depth in the hypoechoic fatty tissue was inferior to that of a 35-MHz transducer. However, this capability of distinguishing vascular layer and tissue surroundings is especially attractive for detecting a vulnerable plaque consisting of a lipid pool surrounded by a fibrous cap. An increase in frequency will allow the resolution and contrast to be further improved, which can be achieved using the free-standing film technology. Integration of the transducer element into a catheter-based probe with a rotational shaft is needed for future animal study or clinical use, but this could be easily realized because the element size is well within the catheter size restriction. Moreover, by designing better customized electronics and integrating time-gain compensation or coded excitation techniques, penetration depth could be further improved.

Acknowledgments

References

[1] B. N. Potkin, A. L. Bartorelli, J. M. Gessert, R. F. Neville, Y. Almagor, W. C. Roberts, and M. B. Leon, "Coronary artery imaging with intravascular high-frequency ultrasound," *Circulation*, vol. 81, no. 5, pp. 1575–1585, 1990.

[2] S. E. Nissen and P. Yock, "Intravascular ultrasound novel pathophysiological insights and current clinical applications," *Circulation*, vol. 103, no. 4, pp. 604–616, 2001.

[3] F. S. Foster, C. J. Pavlin, K. A. Harasiewicz, D. A. Christopher, and D. H. Turnbull, "Advances in ultrasound biomicroscopy," *Ultrasound Med. Biol.*, vol. 26, no. 1, pp. 1–27, 2000.

[4] F. Prati, E. Arbustini, A. Labellarte, B. D. Bello, L. Sommariva, M. T. Mallus, A. Pagano, and A. Boccanelli, "Correlation between high frequency intravascular ultrasound and histomorphology in human coronary arteries," *Heart*, vol. 85, no. 5, pp. 567–570, 2001.

[5] P. Patwari, N. J. Weissman, S. A. Boppart, C. Jesser, D. Stamper, J. G. Fujimoto, and M. E. Brezinski, "Assessment of coronary plaque with optical coherence tomography and high-frequency ultrasound," *Am. J. Cardiol.*, vol. 85, no. 5, pp. 641–644, 2000.

[6] M. E. Brezinski, G. J. Tearney, N. J. Weissman, S. A. Boppart, B. E. Bouma, M. R. Hee, A. E. Weyman, E. A. Swanson, J. F. Southern, and J. G. Fujimoto, "Assessing atherosclerotic plaque morphology: Comparison of optical coherence tomography and high frequency intravascular ultrasound," *Heart*, vol. 77, no. 5, pp. 397–403, 1997.

[7] M. Kawasaki, B. E. Bouma, J. Bressner, S. L. Houser, S. K. Nadkarni, B. D. MacNeill, I. K. Jang, H. Fujiwara, and G. J. Tearney, "Diagnostic accuracy of optical coherence tomography and integrated backscatter intravascular ultrasound images for tissue characterization of human coronary plaques," *J. Am. Coll. Cardiol.*, vol. 48, no. 1, pp. 81–88, 2006.

[8] T. Sawada, J. Shite, H. M. Garcia-Garcia, T. Shinke, S. Watanabe, H. Otake, D. Matsumoto, Y. Tanino, D. Ogasawara, H. Kawamori, H. Kato, N. Miyoshi, M. Yokoyama, P. W. Serruys, and K. Hirata, "Feasibility of combined use of intravascular ultrasound radiofrequency data analysis and optical coherence tomography for detecting thin-cap fibroatheroma," *Eur. Heart J.*, vol. 29, no. 9, pp. 1136–1146, 2008.

[9] J. M. Cannata, T. A. Ritter, W. H. Chen, R. H. Silverman, and K. K. Shung, "Design of efficient, broadband single-element (20–80 MHz) ultrasonic transducers for medical imaging applications," *IEEE Trans. Ultrason. Ferroelectr. Freq. Control*, vol. 50, no. 11, pp. 1548–1557, 2003.

[10] M. Kosec, J. Holc, D. Kuscer, and S. Drnovšek, "Pb(Mg$_{1/3}$Nb$_{2/3}$)O$_3$-PbTiO$_3$ thick films for mechanochemically synthesized powder," *J. Eur. Ceram. Soc.*, vol. 27, no. 13–15, pp. 3775–3778, 2007.

[11] M. L. Calzada, M. Alguero, A. Santos, M. Stewart, M. G. Cain, and L. Pardo, "Piezoelectric, ferroelectric Pb(Mg$_{1/3}$Nb$_{2/3}$)O$_3$–PbTiO$_3$ thin films with compositions around the morphotropic phase boundary prepared by a sol-gel process of reduced thermal budget," *J. Mater. Res.*, vol. 24, no. 2, pp. 526–533, 2009.

[12] H. J. Lee, S. Zhang, J. Luo, F. Li, and T. R. Shrout, "Thickness-dependent properties of relaxor-PbTiO$_3$ ferroelectrics for ultrasonic transducers," *Adv. Funct. Mater.*, vol. 20, no. 18, pp. 3154–3162, 2010.

[13] J. M. Cannata, J. A. Williams, Q. F. Zhou, L. Sun, K. K. Shung, H. Yu, and E. S. Kim, "Self-focused ZnO transducers for ultrasonic biomicroscopy," *J. Appl. Phys.*, vol. 103, no. 8, art. no. 084109, 2008.

[14] B. P. Zhu, D. W. Wu, Q. F. Zhou, J. Shi, and K. K. Shung, "Lead zirconate titanate thick film with enhanced electrical properties for high frequency transducer applications," *Appl. Phys. Lett.*, vol. 93, no. 1, art. no. 012905, 2008.

[15] B. P. Zhu, Q. F. Zhou, J. Shi, K. K. Shung, S. Irisawa, and S. Takeuchi, "Self-separated hydrothermal lead zirconate titanate thick films for high frequency transducer applications," *Appl. Phys. Lett.*, vol. 94, no. 10, art. no. 102901, 2009.

[16] Q. F. Zhou, S. T. Lau, D. W. Wu, and K. K. Shung, "Piezoelectric films for high frequency ultrasonic transducers in biomedical applications," *Prog. Mater. Sci.*, vol. 56, no. 2, pp. 139–174, 2011.

[17] H. Luo, W. Y. Shih, and W.-H. Shih, "Double precursor solution coating approach for low-temperature sintering of [Pb(Mg$_{1/3}$Nb$_{2/3}$)O$_3$]0.63[PbTiO$_3$]0.37 solids," *J. Am. Ceram. Soc.*, vol. 90, no. 12, pp. 3825–3829, 2007.

[18] D. Kuščer, M. Skalar, J. Holc, and M. Kosec, "Processing and properties of 0.65Pb(Mg$_{1/3}$Nb$_{2/3}$)O$_3$–0.35PbTiO$_3$ thick films," *J. Eur. Ceram. Soc.*, vol. 29, no. 1, pp. 105–113, 2009.

[19] H. Uršič, M. Škarabot, M. Hrovat, J. Holc, M. Skalar, V. Bobnar, M. Kosec, and I. Muševič, "The electrostrictive effect in ferroelectric $0.65Pb(Mg_{1/3}Nb_{2/3})O_3$–$0.35PbTiO_3$ thick films," *J. Appl. Phys.*, vol. 103, no. 12, art. no. 124101, 2008.

[20] M. L. Calzada, M. Alguero, J. Ricote, A. Santos, and L. Pardo, "Preliminary results on sol-gel processing of $\langle 100 \rangle$ oriented $Pb(Mg_{1/3}Nb_{2/3})O_3$–$PbTiO_3$ thin films using diol-based solutions," *J. Sol-Gel Sci. Technol.*, vol. 42, no. 3, pp. 331–336, 2007.

[21] W. Y. Shih, H. Luo, C. Martorano, H. Li, and W.-H. Shih, "Sheet geometry enhanced giant piezoelectric coefficients," *Appl. Phys. Lett.*, vol. 89, vol. 24, pp. 242913, 2006.

Xiang Li received a B.E. degree from Zhejiang University, China, in 2007 and a B.S. degree from the University of Southern California (USC), Los Angeles, CA, in 2010. He is currently a Ph.D. candidate in the Department of Biomedical Engineering at USC. He started his Ph.D. studies in 2008 under the support of the USC Provost's Fellowship. In 2010, he won the Student Paper Competition Award at the IEEE International Ultrasonics Symposium, San Diego, CA. Under the direction of Dr. Qifa Zhou and Dr. K. Kirk Shung, Xiang is conducting his research in the NIH Ultrasonic Transducer Resource Center (UTRC) on high-frequency ultrasonic transducer technology, integrated IVUS-OCT imaging, and intravascular photoacoustic imaging.

Wei Wu is a Ph.D. candidate in the Department of Materials Science and Engineering at Drexel University. He graduated with a bachelor's degree in materials science and engineering from the University of Science and Technology of China in 2007, including participating in a summer research program of the Institute of Chemistry at the Chinese Academy of Science in Beijing, China. His research interests and activities include processing of lead magnesium niobate-lead titanate (PMN-PT) powder and freestanding films ranging from 8 to 150 µm in thickness. By controlling the sintering conditions and investigating the microstructure's relationship with properties, he optimized the piezoelectric property of PMN-PT for applications in ultrasonic transducers and biosensors. He made micro-piezoelectric plate cantilever sensors (PEPS) using these optimized good-quality PMN-PT freestanding films; they were used to carry out real-time protein and DNA hybridization detection at ultra-low concentrations for potential early-stage diagnosis, which gives these sensors good potential as portable and inexpensive medical sensors in the future.

Youngsoo Chung earned his Ph.D. degree at the Tokyo Institute of Technology, Tokyo, Japan, in 1991. Before he joined Drexel University as a visiting professor in 2006, he had been working at universities and companies in Korea. Throughout his career of 30 years as a ceramic engineer, he has been researching new technologies, new materials, and new products.

Wan Y. Shih is an associate professor in the School of Biomedical Engineering, Science, and Health Systems at Drexel University. She received her B.S. degree in physics in 1976 from Tsing-Hua University in Taiwan and her Ph.D. degree in physics in 1984 from Ohio State University. She was a Research Scientist in the Department of Materials Science and Engineering at the University of Washington from 1985 to 1993. She was a Research Scientist in the Princeton Institute of Materials at Princeton University from 1993 to 2000 and a Research Associate Professor in the Department of Materials Science and Engineering at Drexel University from 1993 to 2006. She joined the School of Biomedical Engineering, Science, and Health Systems at Drexel University in 2006. Her research has covered a wide range of areas such as superconductivity, colloids, ceramics, piezoelectric materials and devices, and semiconducting nanoparticles. Her recent focus is on the biomedical applications of piezoelectric devices and photoluminescent semiconducting nanoparticles. She received the American Ceramic Society's 1999 Edward C. Henry Electronics Division Best Paper Award for her work in the fundamental understanding of piezoelectric unimorph cantilevers and disks.

Wei-Heng Shih is a professor in the Department of Materials Science and Engineering at Drexel University. He received a B.Sc. in physics in 1976 from Tsing-Hua University in Taiwan and completed his Ph.D. degree in physics in 1984 from Ohio State University. After postdoctoral research at the University of Washington in the Physics Department and the Materials Science and Engineering Department, he joined Drexel University in 1991. His research has covered a wide range of areas of materials science and engineering, including surface modification of powders by colloidal coating, sol-gel processing of microporous and mesoporous powders, low-temperature processing of perovskite piezoelectric ceramics, and fabrication of piezoelectric sensors. He has received the American Ceramic Society's 1999 Edward C. Henry Electronics Division Best Paper Award and the Drexel's Research Achievement Award. His current research focuses on the development of aqueous synthesis of nanocrystalline quantum dots, highly piezoelectric freestanding films, and lead-free piezoelectric ceramics for imaging and sensor applications.

Qifa Zhou received his Ph.D degree from the Department of Electronic Materials and Engineering at Xi'an Jiaotong University, China, in 1993. He is currently a Research Professor at the NIH Resource on Medical Ultrasonic Transducer Technology and the Department of Biomedical Engineering at the University of Southern California (USC), Los Angeles, CA. Before joining USC in 2002, he worked in the Department of Physics at Zhongshan University of China, the Department of Applied Physics at Hong Kong Polytechnic University, and the Materials Research Laboratory at The Pennsylvania State University.

Dr. Zhou is a senior member of IEEE (UFFC Society) and a member of the UFFC Society's Ferroelectric Committee. He is also a member of the Technical Program Committee of the IEEE International Ultrasonics Symposium. He is an Associate Editor of the *IEEE Transactions on Ultrasonics, Ferroelectrics, and Frequency Control*. His current research interests include the development of ferroelectric thin films, MEMS technology, nano-composites, modeling and fabrication of high-frequency ultrasound transducers and arrays for medical imaging applications, and photoacoustic imaging. He has published more than 100 papers in this area.

K. Kirk Shung obtained a B.S. degree in electrical engineering from Cheng-Kung University in Taiwan in 1968, an M.S. degree in electrical engineering from the University of Missouri, Columbia, MO, in 1970, and a Ph.D. degree in electrical engineering from the University of Washington, Seattle, WA, in 1975. He taught at The Pennsylvania State University, University Park, PA, for 23 years before moving to the Department of Biomedical Engineering, University of Southern California, Los Angeles, CA, as a professor in 2002. He has been the director of the NIH Resource on Medical Ultrasonic Transducer Technology since 1997.

Dr. Shung is a Life Fellow of IEEE and a fellow of the Acoustical Society of America and the American Institute of Ultrasound in Medicine. He is a founding fellow of the American Institute of Medical and Biological Engineering. He received the IEEE Engineering in Medicine and Biology Society Early Career Award in 1985 and was the coauthor of a paper that received the best paper award for the *IEEE Transactions on Ultrasonics, Ferroelectrics, and Frequency Control* (UFFC) in 2000. He was elected an outstanding alumnus of Cheng-Kung University in Taiwan in 2001. He was selected as the distinguished lecturer for the IEEE UFFC society for 2002–2003. He received the Holmes Pioneer Award in Basic Science from the American Institute of Ultrasound in Medicine in 2010. He was selected to receive the academic career achievement award from the IEEE Engineering in Medicine and Biology Society in 2011.

Dr. Shung has published more than 400 papers and book chapters. He is the author of the textbook *Principles of Medical Imaging* published by Academic Press in 1992 and the textbook *Diagnostic Ultrasound: Imaging and Blood Flow Measurements* published by CRC press in 2005. He co-edited the book *Ultrasonic Scattering by Biological Tissues* published by CRC Press in 1993. Dr. Shung's research interest is in ultrasonic transducers, high-frequency ultrasonic imaging, ultrasound microbeams, and ultrasonic scattering in tissues.